

Efficient implementation of the superposition of atomic potentials initial guess for electronic structure calculations in Gaussian basis sets

Susi Lehtola,^{1, a)} Lucas Visscher,^{2, b)} and Eberhard Engel³

¹⁾*Department of Chemistry, University of Helsinki, P.O. Box 55 (A. I. Virtasen aukio 1), FI-00014 Helsinki, Finland.*

²⁾*Division of Theoretical Chemistry, Vrije Universiteit Amsterdam, De Boelelaan 1083, 1081 HV Amsterdam, The Netherlands.*

³⁾*Center for Scientific Computing, J. W. Goethe-Universität Frankfurt, Max-von-Laue-Strasse 1, D-60438 Frankfurt am Main, Germany.*

The superposition of atomic potentials (SAP) approach has recently been shown to be a simple and efficient way to initialize electronic structure calculations [S. Lehtola, *J. Chem. Theory Comput.* 15, 1593 (2019)]. Here, we study the differences between effective potentials from fully numerical density functional and optimized effective potential calculations for fixed configurations. We find that the differences are small, overall, and choose exchange-only potentials at the local density approximation level of theory computed on top of Hartree–Fock densities as a good compromise. The differences between potentials arising from different atomic configurations are also found to be small at this level of theory.

Furthermore, we discuss the efficient Gaussian-basis implementation of SAP via error function fits to fully numerical atomic radial potentials. The guess obtained from the fitted potentials can be easily implemented in any Gaussian-basis quantum chemistry code in terms of two-electron integrals. Fits covering the whole periodic table from H to Og are reported for non-relativistic as well as fully relativistic four-component calculations that have been carried out with fully numerical approaches.

I. INTRODUCTION

In order to perform an electronic structure calculation, an initial guess is necessary for the one-particle states *i.e.* orbitals, and several types of guesses have been proposed over the years.¹ The focus of the present work is the superposition of atomic potentials (SAP), which is arguably a very old idea with roots dating back at least to the late 1960s.^{2,3} However, SAP was apparently forgotten for a long time, assumedly due to issues that were only recently fully resolved.¹

But, if one is interested only in Gaussian-basis calculations, then adopting an atomic potential arising from a spherically symmetric Gaussian expansion of a fictitious electron density (yielding error functions as is well-known) leads to facile evaluation of the necessary matrix elements. The formation of the guess reduces to the same two-electron integrals that are used in the subsequent self-consistent field (SCF) procedure, which thus already exist in all Gaussian-basis quantum chemistry programs. Such special variants of the SAP guess were proposed by Whitten and coworkers.^{4–6} They developed potentials derived from Gaussian pseudo-electron densities, which were optimized for specific elements described with a specific Gaussian orbital basis set, and embedded in specific chemical environments.^{4–6}

In contrast to the Gaussian-basis approach pursued by Whitten and coworkers, where the potentials are tailored to specific chemical environments, a parameter-free variant of the SAP guess based on potentials that are

determined from fully numerical⁷ atomic density functional calculations at the complete basis set limit was presented in ref. 1. The resulting SAP guess proved to be the most accurate out of the seven types of initial guesses considered in ref. 1, judged by the projection of the guess orbitals onto the SCF solution. An improved method for determining the atomic potentials necessary for the procedure has been recently presented in ref. 8. A straightforward extension of the work in refs. 1 and 4 has also been recently suggested in ref. 9, in which a universal atomic potential is employed as in ref. 1, but instead of real-space calculations at the basis set limit the potentials are obtained for a small Gaussian basis set and biased for molecular calculations on the lines of ref. 4. However, the optimization in ref. 9 was restricted to fixing the wrong asymptotic behavior of the optimized effective potential discussed by one of the present authors in ref. 10, and instead of minimizing the resulting guess energy as Whitten and coworkers in refs. 4–6, the procedure of ref. 9 maximizes the overlap of the guess orbitals onto the SCF solution according to the procedure first introduced in ref. 1.

All variants of SAP (including refs. 1–6 and 9) assume that the potential the electrons feel in a molecule can be accurately modeled by a simple sum of atomic potentials. Although potentials optimized for molecular calculations may have benefits, the optimization makes them less general than ones derived from atomic calculations. The transferability of optimized potentials across basis sets is not inherently clear, as the optimizations are typically carried out in small basis sets, and any possible artefacts of the small-basis optimization may only become visible in calculations with extended basis sets, or in applications to large molecules. In contrast, potentials derived strictly from first principles are appealing as they can be

^{a)}Electronic mail: susi.lehtola@alumni.helsinki.fi

^{b)}Electronic mail: l.visscher@vu.nl

routinely obtained at the complete basis set limit, thus guaranteeing transferability between basis sets and large systems.¹ They can also be customized for a specific purpose, if so desired. For instance, spin-polarized orbitals for e.g. antiferromagnetically coupled systems can be obtained straightforwardly by employing alternating potentials on the atoms. If one employs the potential corresponding to the atomic majority spin channel from a numerical atomic structure calculation, the resulting guess orbital will place more density on the atom than if one uses the minority spin potential which is less attractive due to a smaller amount of exchange.

To facilitate the implementation of the first-principles SAP guess described in ref. 1 in Gaussian-basis quantum chemistry programs, in the present work we report error function expansions of atomic effective potentials derived from fully numerical atomic calculations. With these fits, the SAP guess can be implemented in any Gaussian-basis quantum chemistry program in terms of three-center two-electron integrals that are familiar from resolution-of-the-identity methods.¹¹ We would especially like to point out that the implementation of the fitted SAP guess is fully analogous to the computation of the nuclear attraction matrix elements for finite nuclei with Gaussian distributions^{12,13} that is already available in several program packages. An implementation of SAP based on this technique has been available in the DIRAC program since its 2016 release, but it has not yet been described.

The outline of the work is as follows. We will briefly summarize the SAP method in section II. Various parameters of the calculations and the fitting procedures are detailed in section III. Section IV presents fits to both non-relativistic and fully relativistic four-component calculations, which have been obtained with the HELFEM and GRASP programs, respectively. Molecular applications of the potentials are shown in section V. The article concludes with a brief summary and discussion in section VI. Atomic units are used throughout the text.

II. METHOD

A. Superposition of atomic potentials

As the name suggests, the basic idea in the SAP approach is to obtain approximate molecular orbitals from an effective one-particle Hamiltonian (shown here in the non-relativistic case for simplicity)

$$\hat{H} = -\frac{1}{2}\nabla^2 + V^{\text{SAP}}(\mathbf{r}) = -\frac{1}{2}\nabla^2 - \sum_A \frac{Z_A(r_A)}{r_A} \quad (1)$$

where the effective potential $V^{\text{SAP}}(\mathbf{r})$ is obtained as a superposition of atomic potentials. The atomic potentials can in turn be rewritten in terms of effective nuclear charges Z_A , as seen at a distance $r_A = |\mathbf{r} - \mathbf{R}_A|$ away from the nucleus A at \mathbf{R}_A . As the potentials V^{SAP} are to be local, we will define the exchange-(correlation) part

of the potential in terms of density functional approximations (DFA) to density functional theory^{14,15} (DFT) as in ref. 1.

Due to the radial dependence of the effective charge, the reliable calculation of the matrix elements of the Hamiltonian in equation (1) appears difficult. However, the realization made in ref. 1 was that similar numerical problems also appear in density functional approaches; for example, the multicenter quadrature scheme of ref. 16 is a suitable solution in the case of atomic basis set calculations. The matrix elements of equation (1) can be computed by minor modifications to existing density functional routines; such implementations are now available in ERKALE,^{17,18} PSI4,¹⁹ and the fully numerical HELFEM program.^{20–22} (A similar approach has also been used in the calculation of matrix elements for the “maximum of atomic potentials” approach to the zeroth-order regular expansion approximation²³ within the ADF program.²⁴)

In contrast, the implementation in DIRAC, like the work in refs. 4–6 and 9, is based on expanding the electronic part of the radial potential in terms of the potentials of primitive normalized s -type Gaussians $g_p(r) = (\alpha_p/\pi)^{3/2} \exp(-\alpha_p r^2)$ that have the simple expression²⁵ $V_p(r) = \text{erf}(\sqrt{\alpha_p}r)/r$, where erf is the error function. The comparison of equation (1) to the above shows that this amounts simply to expanding $Z^{\text{el}}(r)$ in a set of error functions $\phi_p^0 = \text{erf}(\beta_p r)$ with arguments $\beta_p = \sqrt{\alpha_p}$ and expansion coefficients $\{c_p\}_{p=1}^N$. The matrix elements of the fitted potential in an atom-centered orbital basis $\{\chi_i\}$

$$V_{ij}^{\text{el}} = \langle i|V|j \rangle = \int \chi_i(\mathbf{r})V(r_A)\chi_j(\mathbf{r})d^3r \quad (2)$$

become easy to evaluate, as rewriting the error functions in integral form as potentials arising from the normalized Gaussian functions $|\alpha_p\rangle$ yields an expression in terms of three-center two-electron integrals (3C-TEIs)

$$V_{ij}^{\text{el}} = - \sum_{p=1}^N c_p (ij|\alpha_p), \quad (3)$$

where the negative sign comes from equation (1). 3C-TEIs are familiar from resolution-of-the-identity methods.¹¹ Equation (3) also bears a strong similarity to the description of finite nuclei with Gaussian distributions in quantum chemical calculations,^{12,13} where only a single auxiliary function α is used; its exponent being determined by the size of the nucleus and its coefficient coinciding with the nuclear charge.

3C-TEIs can be obtained as a special case of general two-electron integrals—the basic ingredient of Gaussian-basis quantum chemistry programs—that can be evaluated analytically in an efficient fashion;^{26,27} alternatively, 3C-TEIs can be evaluated even more efficiently with specialized approaches.²⁸ The (approximate) fit of the radial potential thereby allows one to circumvent the need for (approximate) quadratures of $V(r)$ pursued in ref. 1.

B. Fitting scheme

The fitting error with fitting coefficients $\{c_p\}$ and a fitting basis $\{\phi_p^0\}$ is given by

$$\tau = \int_0^\infty \left[Z^{\text{el}}(r) - \sum_p c_p \phi_p^0(r) \right]^2 dr. \quad (4)$$

Although error functions were adopted as the fitting basis in section II A, a complication with this choice is that the overlap matrix

$$S_{pq}^0 = \int_0^\infty \phi_p^0(r) \phi_q^0(r) dr \quad (5)$$

is divergent. In order to determine the coefficients, it is therefore better to rewrite the problem in terms of complementary error functions. Taking $\phi_p(r) = \text{erfc}(\beta_p r)$ leads to an analytical expression for the overlap matrix

$$S_{pq} = \frac{\beta_p + \beta_q - \sqrt{\beta_p^2 + \beta_q^2}}{\beta_p \beta_q \sqrt{\pi}}, \quad (6)$$

meaning that such a basis is well-behaved for an expansion. All that remains is to rewrite the original fitting problem in terms of erfc 's. As $\phi_p^0(r) = \text{erf}(\beta_p r) = 1 - \text{erfc}(\beta_p r) = 1 - \phi_p(r)$, equation (4) can be rewritten as

$$\tau = \int_0^\infty \left[\left(Z^{\text{el}}(r) - \sum_p c_p \right) + \sum_p c_p \phi_p(r) \right]^2 dr \quad (7)$$

without changing the meaning of the coefficients c_p .

The DFA potentials used in the present work have the important property that far away the effective charge goes to zero,¹ $Z_A(\infty) = Z_A - Z_A^{\text{el}}(\infty) = 0$. Imposing this long-range limit translates into the condition

$$\sum_p c_p = -Z \quad (8)$$

where Z is the nuclear charge. (Note that atomic potentials that do not satisfy this requirement lead to molecular potentials that become worse and worse in increasing system size, see the discussion in ref. 10.)

Furthermore, we can rewrite equation (7) in terms of an effective charge as $Z(r) = Z - Z^{\text{el}}(r)$ by using equation (8). This redefinition of $Z(r)$ coincides with the screened nuclear potential in the case of a point nucleus, but this mathematical trick works equally well with a finite nucleus: the important thing to notice here is that the nuclear model does not enter into the fits of the potential generated by the electrons. Equation (7) thus becomes

$$\tau = \int_0^\infty \left[Z(r) - \sum_p c_p \phi_p(r) \right]^2 dr. \quad (9)$$

Although equation (9) already allows fits to the redefined $Z(r)$, these fits may still violate the charge neutrality condition, equation (8). The condition can be enforced by treating the coefficient of the steepest function as a dependent variable

$$c_n = Z - \sum_{p=1}^{n-1} c_p, \quad (10)$$

so that the fitting problem for the $n - 1$ remaining coefficients becomes

$$\begin{aligned} \tau &= \int_0^\infty \left[[Z(r) - Z\phi_n(r)] - \sum_{p=1}^{n-1} c_p [\phi_p(r) - \phi_n(r)] \right]^2 dr \\ &= \int_0^\infty \left[\tilde{Z}(r) - \sum_{p=1}^{n-1} c_p \tilde{\phi}_p(r) \right]^2 dr. \end{aligned} \quad (11)$$

The error is minimized by coefficients \mathbf{c} that satisfy

$$\frac{\partial \tau}{\partial c_q} = -2 \int_0^\infty \left[\tilde{Z}(r) - \sum_p c_p \tilde{\phi}_p(r) \right] \tilde{\phi}_q(r) dr = 0 \quad (12)$$

from which

$$\tilde{\mathbf{S}} \mathbf{c} = \tilde{\mathbf{Z}}, \quad (13)$$

where

$$\tilde{Z}_q = \int_0^\infty \tilde{Z}(r) \tilde{\phi}_q(r) dr \quad (14)$$

$$\tilde{S}_{pq} = \int_0^\infty \tilde{\phi}_p(r) \tilde{\phi}_q(r) dr. \quad (15)$$

Equation (13) can be solved for the $n - 1$ coefficients, *e.g.*, by computing the inverse overlap matrix via the canonical orthogonalization procedure²⁹ in which eigenvectors with eigenvalues smaller than 10^{-7} are omitted, after which the dependent coefficient is calculated from equation (10). The basis set is normalized before the canonical orthogonalization procedure to ensure proper conditioning of the eigenproblem.³⁰ While one may in principle define any coefficient as the dependent coefficient, eliminating the coefficient of the tightest function has the advantage that the function $\tilde{Z}(r) = Z(r) - Z\phi_n(r)$ exhibits the fastest decay to zero for $r \rightarrow 0$.

The function $Z(r)$ from HELFEM or GRASP is essentially exact: it yields the energy of the atom at the complete basis set limit. Also the matrix elements of equation (14) can be evaluated exactly, *i.e.* without any significant error, with the numerical grid from HELFEM or GRASP, since $Z(r)$ is accurately known where it is non-zero. The overlap integrals of equation (15), in turn, are evaluated analytically via equation (6). The only potentially significant source of numerical errors in the fitting procedure is the calculation of the total fit error τ in equation (4), as this quantity may not be evaluated accurately by quadrature on the grid.

Especially, the grid is deficient in regions where $Z(r) = 0$, that is, far away from the nucleus: although the fit coefficients are accurately evaluated, the resulting fit error is not. For instance, if the most diffuse fitting functions are nonzero at the practical infinity r_∞ of the fully numerical calculation, $\text{erfc}(\beta_{\min} r_\infty) \neq 0$, the fit error in the potential from $r = r_\infty$ to $r = \infty$ is completely neglected by the quadrature. A more accurate evaluation of the fitting error τ can be achieved by the addition of a penalty term

$$\tau \rightarrow \tau + \sum_{pq} c_p [S_{pq} - \tilde{S}_{pq}] c_q \quad (16)$$

where \tilde{S} is the quadrature evaluation of the overlap matrix. Fit functions that are accurately described on the grid carry no penalty as $\tilde{S}_{pq} \approx S_{pq}$. Otherwise, the fit functions pick up a penalty, as they should: if the functions are not accurately described on the grid, their form also ill describes $Z(r)$, whose grid representation is known to be exact. This means that in addition to describing the quadrature error in (r_∞, ∞) discussed above, the term may also describe quadrature errors in $(0, r_\infty)$.

The linear expansion coefficients c_p are unambiguously determined by equations (13) to (15) once the primitives β_p have been chosen. For simplicity, we use a universal set of even-tempered parameters $\beta_p = \beta_0 \gamma^p$ where β_0 and γ are constants and p are integers, as such expansions afford an easy way to approach the complete (fitting) basis set limit.³¹ The actual procedure for the formation of the fitting basis follows the procedure of ref. 32. First, the best single β_p parameter is found (also allowing negative values of p), after which steeper and more diffuse functions are added into the fitting basis set one by one until the complete fitting-basis-set limit has been achieved, defined as the point at which the fit error only goes up when further functions are added due to finite numerical accuracy. Next, because the fit error often plateaus long before the minimum error for the given β_0 and γ is found, the shortest expansion that yields an error within 5% of the minimum is chosen for production purposes.

However, this set of fits that yields (close to) the lowest possible error for each element with given β_0 and γ is still suboptimal, as fixed values for β_0 and γ afford fits of a different quality for different elements in the periodic table. The fit error τ can be made especially small for the lightest elements, while the error tends to increase with Z . A balanced fit has a uniform accuracy across Z ; this is achieved by truncating the fits further so that $\tau'(Z) \leq \max_Z \tau(Z)$ still holds, that is, so that the fit error of the truncated fits $\tau'(Z)$ is bound by the largest error of the original fits $\tau(Z)$. The truncation results in a major compactification of the tabulated fits by reducing the fits for the light elements to a fraction of their original size.

III. COMPUTATIONAL DETAILS

Non-relativistic calculations were performed with HELFEM^{8,20,21} using 20 radial elements and a value of the practical infinity $r_\infty = 40a_0$; the resulting HELFEM energies are converged beyond nanohartree accuracy for all atoms.^{8,21} The HELFEM calculations employed fractional occupations resulting in spherically symmetric densities, and the ground state for each element was found automatically by a brute force search,⁸ leading *e.g.* to the unrestricted Hartree–Fock (HF) configurations shown in table I. The equations for calculating the radial potential in the finite element formalism used in HELFEM have been presented in ref. 8 to which we refer for further details.

The relativistic calculations were carried out with a modified version³³ of GRASP³⁴ using the settings described in ref. 12; in short, the Gaussian nuclear model¹² was used in combination with the average level (AL) option of GRASP to provide a balanced description of the valence levels. The resulting Hartree–Fock total and orbital energies have been presented in ref. 12.

In order to study the accuracy of the density functional potentials, optimized effective potential (OEP) calculations were performed as detailed in ref. 35. Both the non-relativistic radial Kohn–Sham equations and the OEP integral equation for the exact exchange potential were solved fully numerically on a logarithmic radial grid containing 4000 points to obtain high accuracy. The Krieger–Li–Iafrate identity³⁶ was applied for the normalization of the exchange potential. In the case of open spin-subshells, the spin-up and spin-down Kohn–Sham potentials were averaged.

IV. RESULTS

A. Form of the potential

In order to select the form of the radial potential, we study the Fe atom in its $4s^2 3d^6$ quintet ground state. Because the state should exhibit significant spin-polarization, it should serve well to illustrate differences in the possible choices for the radial potential. We will restrict the present study to exchange-only calculations, since the best results in ref. 1 were obtained with exchange-only potentials.

Four kinds of calculations were performed with HELFEM with fractional occupations, using the methodology presented in ref. 8. The first three are fully self-consistent calculations with exchange either described by the local density approximation (LDA),^{37,38} the PBE³⁹ functional, or the EV93⁴⁰ functional; PBE and EV93 are both generalized gradient functionals. The fourth is a hybrid procedure in which the orbitals are determined by a fractionally occupied Hartree–Fock calculation, after which a (non-self-consistent) radial potential is calculated with the LDA exchange functional; this scheme will be

| | n_s | n_p | n_d | n_f | E/E_h | M | | n_s | n_p | n_d | n_f | E/E_h | M | | n_s | n_p | n_d | n_f | E/E_h | M |
|----|-------|-------|-------|-------|--------------|-----|----|-------|-------|-------|-------|---------------|-----|----|-------|-------|-------|-------|---------------|-----|
| H | 1 | 0 | 0 | 0 | -0.500000 | 2 | Nb | 8 | 18 | 15 | 0 | -3753.558738 | 6 | Tl | 12 | 25 | 30 | 14 | -18961.760416 | 2 |
| He | 2 | 0 | 0 | 0 | -2.861680 | 1 | Mo | 9 | 18 | 15 | 0 | -3975.552980 | 7 | Pb | 11 | 27 | 30 | 14 | -19523.935177 | 5 |
| Li | 3 | 0 | 0 | 0 | -7.432751 | 2 | Tc | 10 | 18 | 15 | 0 | -4204.794932 | 6 | Bi | 12 | 27 | 30 | 14 | -20095.588624 | 4 |
| Be | 4 | 0 | 0 | 0 | -14.573023 | 1 | Ru | 10 | 18 | 16 | 0 | -4441.293960 | 5 | Po | 12 | 28 | 30 | 14 | -20676.415929 | 3 |
| B | 4 | 1 | 0 | 0 | -24.415026 | 2 | Rh | 8 | 18 | 19 | 0 | -4685.642225 | 2 | At | 12 | 29 | 30 | 14 | -21266.785190 | 2 |
| C | 3 | 3 | 0 | 0 | -37.599255 | 5 | Pd | 8 | 18 | 20 | 0 | -4937.921024 | 1 | Rn | 12 | 30 | 30 | 14 | -21866.772241 | 1 |
| N | 4 | 3 | 0 | 0 | -54.404548 | 4 | Ag | 9 | 18 | 20 | 0 | -5197.698943 | 2 | Fr | 13 | 30 | 30 | 14 | -22475.858834 | 2 |
| O | 4 | 4 | 0 | 0 | -74.622399 | 3 | Cd | 10 | 18 | 20 | 0 | -5465.133143 | 1 | Ra | 14 | 30 | 30 | 14 | -23094.303666 | 1 |
| F | 4 | 5 | 0 | 0 | -99.164711 | 2 | In | 10 | 19 | 20 | 0 | -5740.102296 | 2 | Ac | 14 | 30 | 31 | 14 | -23722.088791 | 2 |
| Ne | 4 | 6 | 0 | 0 | -128.547098 | 1 | Sn | 9 | 21 | 20 | 0 | -6022.853866 | 5 | Th | 12 | 30 | 34 | 14 | -24359.586764 | 5 |
| Na | 5 | 6 | 0 | 0 | -161.858954 | 2 | Sb | 10 | 21 | 20 | 0 | -6313.487048 | 4 | Pa | 13 | 30 | 30 | 18 | -25006.654223 | 6 |
| Mg | 6 | 6 | 0 | 0 | -199.614636 | 1 | Te | 10 | 22 | 20 | 0 | -6611.692943 | 3 | U | 12 | 30 | 30 | 20 | -25664.034255 | 7 |
| Al | 6 | 7 | 0 | 0 | -241.803440 | 2 | I | 10 | 23 | 20 | 0 | -6917.876506 | 2 | Np | 12 | 30 | 30 | 21 | -26331.520612 | 8 |
| Si | 5 | 9 | 0 | 0 | -288.763297 | 5 | Xe | 10 | 24 | 20 | 0 | -7232.138364 | 1 | Pu | 13 | 30 | 30 | 21 | -27008.844714 | 9 |
| P | 6 | 9 | 0 | 0 | -340.719275 | 4 | Cs | 11 | 24 | 20 | 0 | -7553.933772 | 2 | Am | 14 | 30 | 30 | 21 | -27695.900612 | 8 |
| S | 6 | 10 | 0 | 0 | -397.386801 | 3 | Ba | 12 | 24 | 20 | 0 | -7883.543827 | 1 | Cm | 14 | 30 | 31 | 21 | -28392.659412 | 9 |
| Cl | 6 | 11 | 0 | 0 | -459.339556 | 2 | La | 12 | 24 | 21 | 0 | -8220.952378 | 2 | Bk | 14 | 30 | 30 | 23 | -29099.513303 | 6 |
| Ar | 6 | 12 | 0 | 0 | -526.817513 | 1 | Ce | 10 | 24 | 24 | 0 | -8566.569397 | 5 | Cf | 13 | 30 | 30 | 25 | -29816.800544 | 5 |
| K | 7 | 12 | 0 | 0 | -599.164870 | 2 | Pr | 12 | 24 | 20 | 3 | -8920.395478 | 4 | Es | 12 | 30 | 30 | 27 | -30544.612534 | 2 |
| Ca | 8 | 12 | 0 | 0 | -676.758186 | 1 | Nd | 11 | 24 | 20 | 5 | -9283.115285 | 7 | Fm | 12 | 30 | 30 | 28 | -31282.870930 | 1 |
| Sc | 8 | 13 | 0 | 0 | -759.574264 | 2 | Pm | 10 | 24 | 20 | 7 | -9654.657927 | 8 | Md | 13 | 30 | 30 | 28 | -32031.172211 | 2 |
| Ti | 7 | 12 | 3 | 0 | -848.081411 | 5 | Sm | 11 | 24 | 20 | 7 | -10034.895222 | 9 | No | 14 | 30 | 30 | 28 | -32789.512140 | 1 |
| V | 6 | 12 | 5 | 0 | -942.764789 | 6 | Eu | 12 | 24 | 20 | 7 | -10423.550567 | 8 | Lr | 14 | 31 | 30 | 28 | -33557.817804 | 2 |
| Cr | 7 | 12 | 5 | 0 | -1043.356782 | 7 | Gd | 12 | 24 | 21 | 7 | -10820.539254 | 9 | Rf | 12 | 30 | 34 | 28 | -34336.517013 | 5 |
| Mn | 8 | 12 | 5 | 0 | -1149.869841 | 6 | Tb | 10 | 24 | 24 | 7 | -11226.259522 | 12 | Db | 12 | 30 | 35 | 28 | -35125.642045 | 6 |
| Fe | 8 | 13 | 5 | 0 | -1262.258941 | 7 | Dy | 12 | 24 | 20 | 10 | -11640.492034 | 5 | Sg | 13 | 30 | 35 | 28 | -35924.911091 | 7 |
| Co | 8 | 12 | 7 | 0 | -1380.935491 | 4 | Ho | 11 | 24 | 20 | 12 | -12064.271314 | 4 | Bh | 14 | 30 | 35 | 28 | -36734.336697 | 6 |
| Ni | 6 | 12 | 10 | 0 | -1506.669759 | 1 | Er | 10 | 24 | 20 | 14 | -12497.495591 | 1 | Hs | 12 | 30 | 38 | 28 | -37553.987931 | 3 |
| Cu | 7 | 12 | 10 | 0 | -1638.964246 | 2 | Tm | 11 | 24 | 20 | 14 | -12940.015784 | 2 | Mt | 12 | 30 | 39 | 28 | -38384.346407 | 2 |
| Zn | 8 | 12 | 10 | 0 | -1777.848116 | 1 | Yb | 12 | 24 | 20 | 14 | -13391.456193 | 1 | Ds | 12 | 30 | 40 | 28 | -39225.264332 | 1 |
| Ga | 8 | 13 | 10 | 0 | -1923.187642 | 2 | Lu | 12 | 25 | 20 | 14 | -13851.703406 | 2 | Rg | 13 | 30 | 40 | 28 | -40076.354892 | 2 |
| Ge | 8 | 14 | 10 | 0 | -2075.267721 | 3 | Hf | 10 | 24 | 24 | 14 | -14321.061494 | 5 | Cn | 14 | 30 | 40 | 28 | -40937.797856 | 1 |
| As | 8 | 15 | 10 | 0 | -2234.239855 | 4 | Ta | 10 | 24 | 25 | 14 | -14799.827000 | 6 | Nh | 14 | 31 | 40 | 28 | -41809.475125 | 2 |
| Se | 8 | 16 | 10 | 0 | -2399.761455 | 3 | W | 11 | 24 | 25 | 14 | -15287.662265 | 7 | Fl | 13 | 33 | 40 | 28 | -42691.604385 | 5 |
| Br | 8 | 17 | 10 | 0 | -2572.317356 | 2 | Re | 12 | 24 | 25 | 14 | -15784.544119 | 6 | Mc | 14 | 33 | 40 | 28 | -43584.201351 | 4 |
| Kr | 8 | 18 | 10 | 0 | -2752.054977 | 1 | Os | 12 | 24 | 26 | 14 | -16290.475039 | 5 | Lv | 14 | 34 | 40 | 28 | -44487.022704 | 3 |
| Rb | 9 | 18 | 10 | 0 | -2938.357567 | 2 | Ir | 10 | 24 | 29 | 14 | -16806.002785 | 2 | Ts | 14 | 35 | 40 | 28 | -45400.387450 | 2 |
| Sr | 10 | 18 | 10 | 0 | -3131.545686 | 1 | Pt | 10 | 24 | 30 | 14 | -17331.121868 | 1 | Og | 14 | 36 | 40 | 28 | -46324.355815 | 1 |
| Y | 10 | 19 | 10 | 0 | -3331.575414 | 2 | Au | 11 | 24 | 30 | 14 | -17865.400624 | 2 | | | | | | | |
| Zr | 8 | 18 | 14 | 0 | -3538.801672 | 5 | Hg | 12 | 24 | 30 | 14 | -18408.991495 | 1 | | | | | | | |

TABLE I. Non-relativistic spin-unrestricted spherical Hartree-Fock configurations used for the HELFEM calculations. Legend: spin multiplicity M , number of s electrons n_s , number of p electrons n_p , number of d electrons n_d , number of f electrons n_f , total energy E . A lower configuration for Lr was found in the brute-force search but it failed to converge, due to which a low-lying excited state is used instead.

denoted LDA@HF for the remainder of the manuscript. The LDA@HF scheme is an example of density-corrected DFT,^{41,42} which sometimes offers a way to obtain more accurate results in DFT calculations.

As is well known, the electronic structure of atoms is dissimilar from that of molecules: atoms often exhibit sig-

nificant spin-polarization, while molecules are typically singlets;⁴³ thus, good performance for atoms does not necessarily imply good behavior for molecules. As a potential that is both local and scalar is desired for use in molecular calculations, we consider four ways in which such a potential can be achieved from an atomic calcu-

lation. We study (i) spin-restricted calculations on the $4s^23d^6$ singlet state, as well as three kinds of potentials from spin-unrestricted calculations on the $4s^23d^6$ quintet state: (ii) the spin-averaged potential, (iii) the potential from the spin-averaged density, as well as (iv) the majority-spin potential.

To begin, we compare the various kinds of density functional potentials against the OEP for a spin-restricted calculation; the results are shown in figure 1. The potentials are indistinguishable until about one bohr, where the density functionals start to diverge from the OEP. The OEP saturates to its asymptotic limit $V(r) = -1/r$ at a distance of 2 bohr, while the density functional potentials keep on decaying exponentially.

The difference of the self-consistent LDA, PBE and EV93 potentials from the non-self-consistent LDA@HF potential is further studied in figure 2. The EV93 potential clearly has a lot more structure than LDA@HF, and is characterized by a number of kinks and sharp peaks. Also the PBE potential is somewhat peaked. The LDA and LDA@HF potentials, however, are close to identical – differing by less than $0.04e$ at any range – implying that self-consistency is not that important.

Next, the spin-averaged and majority-spin potentials from spin-unrestricted calculations are shown in figures 3 and 4, respectively, and the differences of the various DFT potentials from the LDA@HF potential are shown in figures 5 and 6 for the spin-averaged and majority-spin potentials, respectively. All three potentials appear surprisingly similar, from which one can infer that the choice of the density functional has little effect on the potential for a fixed electronic configuration.

The use of a fixed electronic configuration is, however, a restriction: different choices of the functional and of the spin treatment may yield different ground state configurations. Such changes are likely to be reflected as larger changes in the potential, which are not considered here. The optimal electronic configuration to be used for a starting guess in molecular calculations is probably the one that is dominant in a molecular environment. For heavy elements the choice is, however, not straightforward, as they may exhibit many low-lying states that couple strongly together in a molecular environment.

To demonstrate the differences in the potential arising from a change of the reference configuration, in figure 7 we show the differences between the LDA@HF potentials computed for the ground-state $[\text{Xe}]6s^25d^1$ configuration, and the $[\text{Xe}]6s^15d^2$ and $[\text{Xe}]6s^24f^1$ excited-state configurations of lanthanum. These differences are similar in magnitude to those observed between different functionals for Fe in $4s^23d^6$, suggesting that the choice of the reference configuration should also be of relatively small importance for the initial guess.

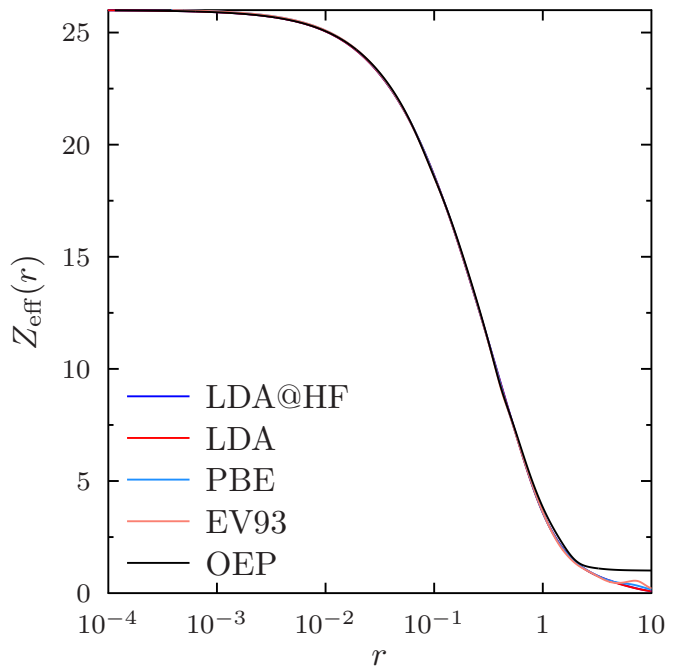


FIG. 1. Spin-restricted potentials for $4s^23d^6$ Fe. The potentials are indistinguishable until about $r = a_0$, where the OEP starts to approach the asymptotic behavior visible at large r .

B. Choice of the potential

We have discussed four different ways in which the effective scalar potential can be chosen from a (possibly spin-polarized) atomic calculation, but it is not *a priori* clear which one affords the best accuracy in molecular calculations due to the characteristic differences between the electronic structure of atoms and molecules. As first-row transition metals have significant open-shell character and spin polarization, and are also infamous for their several low-lying excited atomic configurations, first-row transition metal complexes should offer excellent test cases for determining how the effective atomic radial potential should be formed for molecular calculations.

We employ the quadrature-based implementation of the SAP guess of ref. 1 to assess the four possible choices for the scalar atomic potential, which were outlined above in section IV A. Calculations are performed with ERKALE on the set of 32 diverse first-row transition metal complexes of ref. 44 at the BP86/def2-QZVP^{45–47} level of theory, which yields a good description of the ground-state geometries.⁴⁴ Note that this set also formed part of the test set of ref. 1, in which the SAP guess (based on less accurate radial potentials than in the present work) was assessed in comparison to several other commonly-used initial guesses, and was shown to yield good accuracy. A (75,302) grid was used for the SAP guess and the density functional calculation, and linear interpolation was used for the tabulated potential. The geometries of ref. 44 are

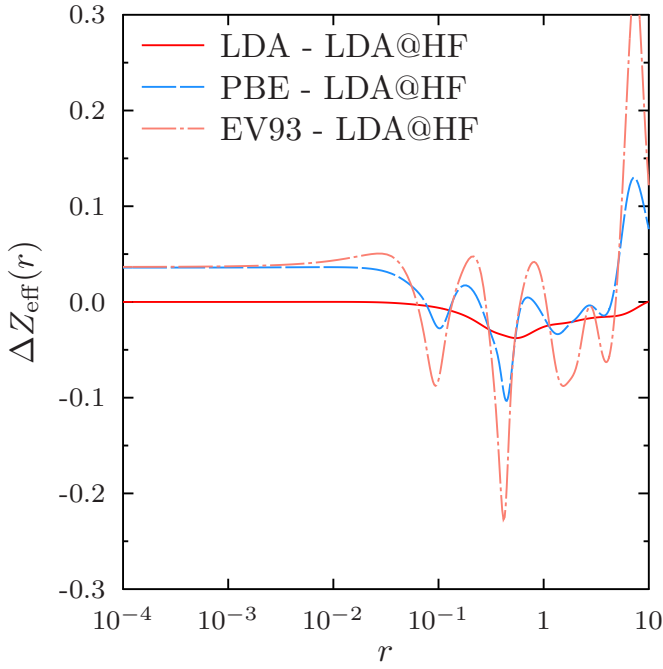


FIG. 2. Difference of spin-restricted potentials for $4s^2 3d^6$ Fe.

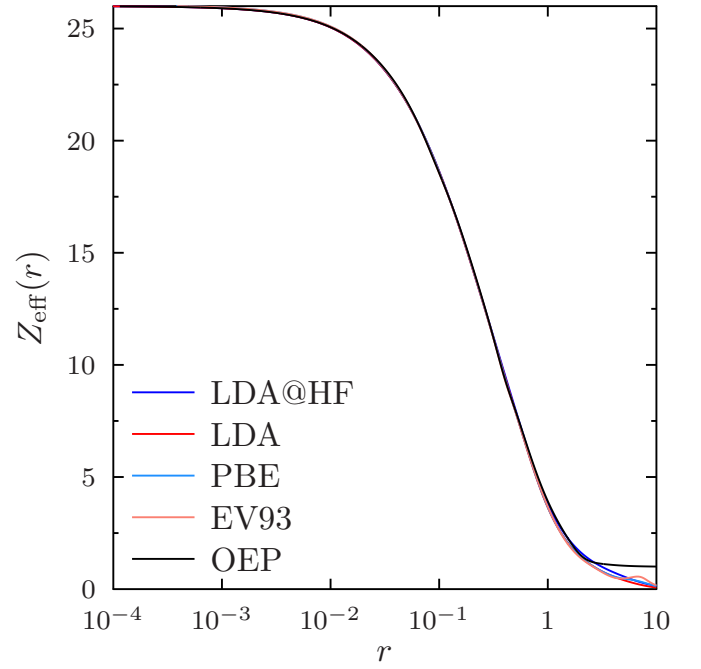


FIG. 4. Majority-spin potentials for $4s^2 3d^6$ Fe.

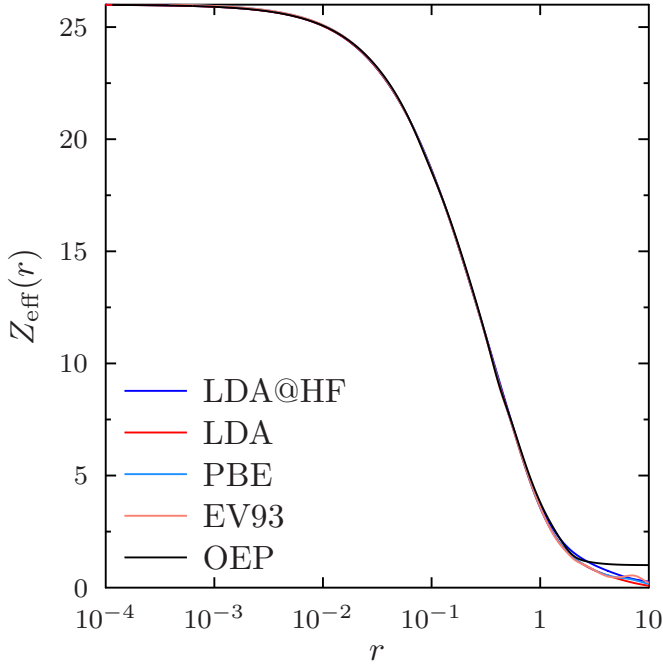


FIG. 3. Spin-averaged potentials for $4s^2 3d^6$ Fe.

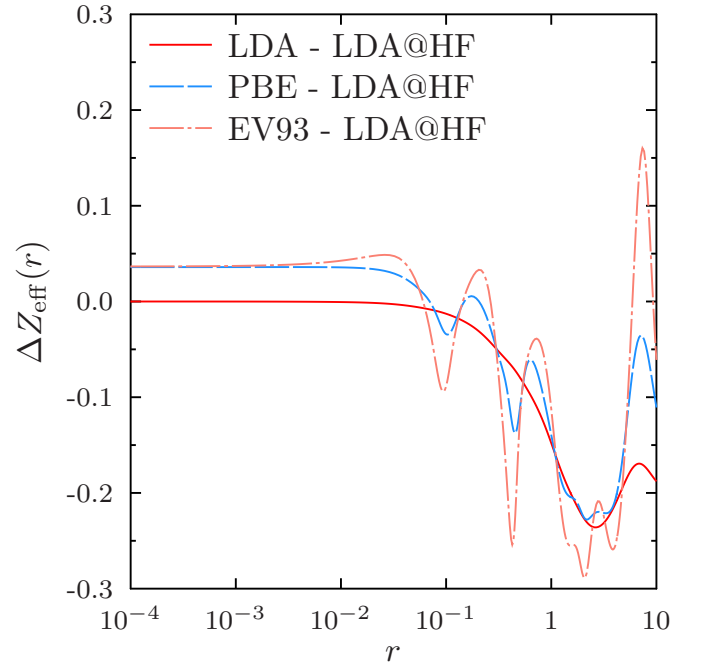


FIG. 5. Difference of spin-averaged potentials for $4s^2 3d^6$ Fe.

used, which are optimal for this level of theory. The universal Coulomb fitting basis set for the def2 series⁴⁸ is used to reduce the cost of the calculations.

The HELFEM potentials corresponding to the four choices of the potential with either LDA or HF orbitals (taken from their corresponding ground state configurations) yield the results in table II. The best re-

sults are obtained with the spin-averaged potential from unrestricted HF calculations, while the potential from the spin-averaged density yields the second-best results. (The unrestricted HF configurations were given above in table I, while the spin-restricted LDA and HF configurations were reported in ref. 8.)

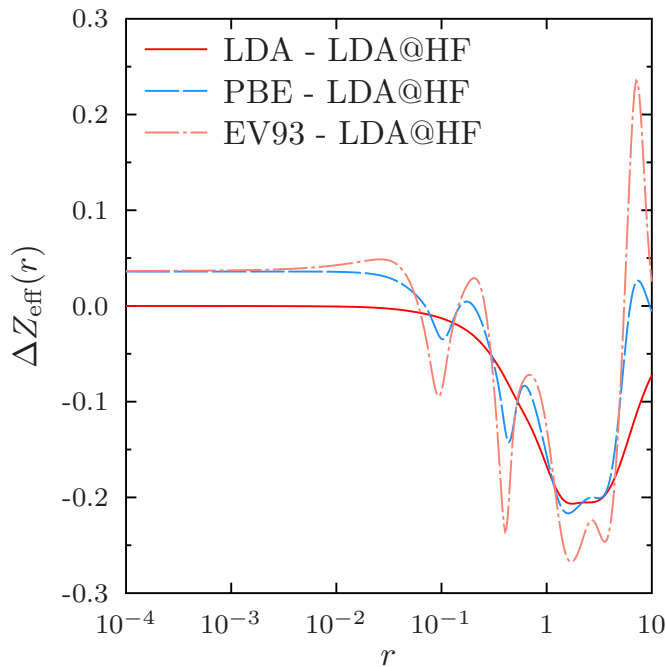


FIG. 6. Difference of majority-spin potentials for $4s^2 3d^6$ Fe.

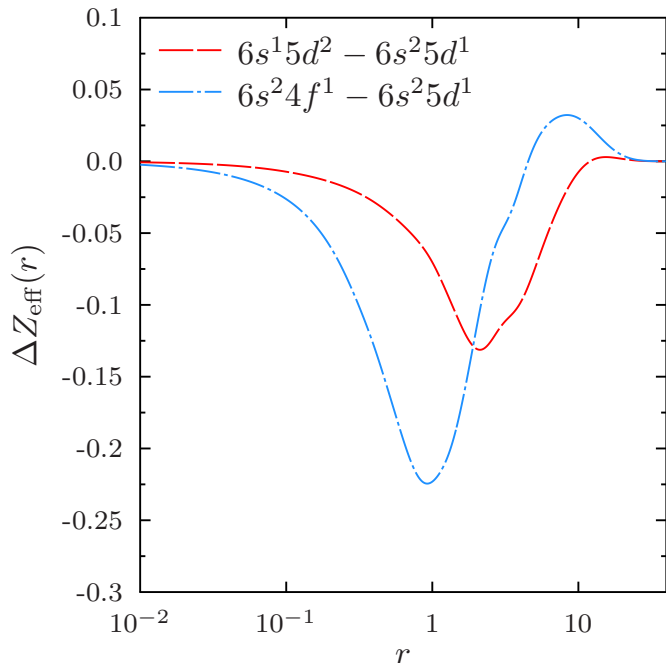


FIG. 7. Difference of configurations for La computed with LDA@HF at the Dirac-Coulomb level of theory with GRASP.

C. Error-function fits of the local exchange potential

Let us summarize the work so far. We found the potentials given by various functionals to be more or less similar for the $4s^2 3d^6$ states of iron in section IV A, so for simplicity we chose to use local exchange potentials

| Potential | Mean error (E_h) |
|--------------|----------------------|
| LDA@HF (ii) | 5.679 |
| LDA (ii) | 7.015 |
| LDA@HF (iii) | 10.011 |
| LDA (iii) | 10.232 |
| LDA (i) | 12.540 |
| LDA (iv) | 14.400 |
| LDA@HF (iv) | 14.518 |
| LDA@HF (i) | 16.428 |

TABLE II. Mean errors in the SAP guess energy for the transition metal complex database of ref. 44 at BP86/def2-QZVP level of theory for various choices of the LDA or LDA@HF potential discussed in section IV A.

for the rest of the work. The local exchange potentials for the various configurations for La were also found to have similar shapes in section IV A, meaning that any reasonable choice for the atomic configurations should yield similar results. Finally, the use of Hartree-Fock orbitals to generate the LDA potentials was found to result in smaller errors of the guess energy in section IV B, due to which Hartree-Fock orbitals are used for the rest of this work.

Relativistic potentials are generated with GRASP from (spin-restricted) average-level Dirac-Coulomb-Hartree-Fock calculations,¹² whereas the non-relativistic potentials from HELFEM are based on spin-unrestricted Hartree-Fock calculations,⁸ as multiconfigurational calculations are not yet available in HELFEM. In order to have a consistent, unambiguous and non-empirical choice of configuration, we choose the configuration with the lowest energy as the reference configuration. That is, the GRASP calculations generate a potential from the configuration with the lowest average energy from the AL calculations, whereas the HELFEM calculations employ the configuration yielding the lowest energy using a spherically symmetric density (table I).

Before full engagement with the error-function fits, we demonstrate that the error function basis is suitable for expanding the radial potential. Figure 8 shows the projections of the radial potentials for the noble gas series produced by HELFEM onto normalized complementary error functions according to equation (14). The similarity of the shape of the projections is striking: even though the nuclear charge ranges from $Z = 2$ for He to $Z = 86$ for Rn, there is but a slight migration to steeper exponents, with a strong decay for the tight region. Due to the smooth behavior evidenced by figure 8, we can start planning the actual fits.

Exploratory calculations were performed on the alkali and noble gas atoms with $\beta_0 = 10^{-2}$ and various choices for γ (1.2, 1.3, ..., 2.0), as the alkali metals and the noble gases represent the most delocalized and the most localized electronic structure, correspondingly. The calculations (not shown) confirm that as expected, the fit error decreases monotonically in decreasing β , and that

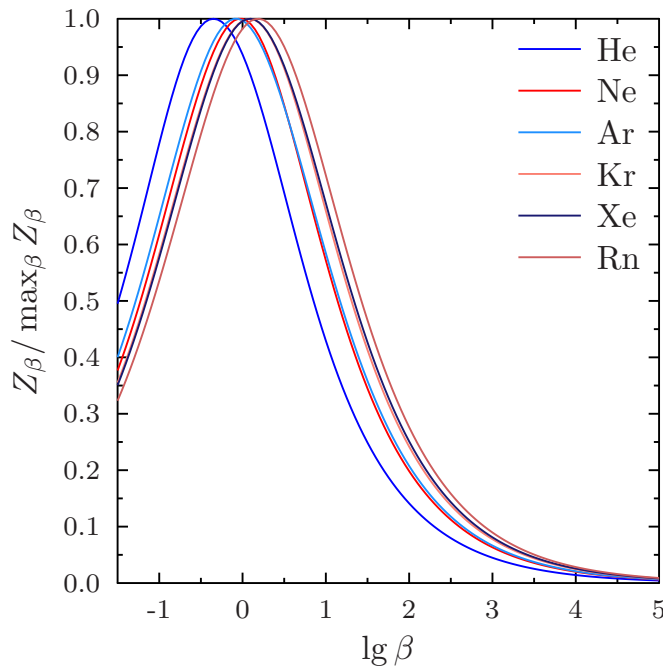


FIG. 8. Projection of $Z(r)$ onto a normalized complementary error function $N(\beta) \text{erfc}(\beta r)$. As these projections still scale with Z , they have been further normalized to a unit maximum for each element.

suitably accurate fits are achievable with $\gamma = 1.4$; this choice corresponds to a spacing of $\gamma^2 = 1.96$ for the density primitives α_p . The choice $\gamma = 1.8$ that corresponds to a density primitive spacing of $\gamma^2 = 3.24$ yields a less accurate but computationally cheaper choice for the fitting basis.

Having fixed the parameters used for the fits, the fits for the whole set of HELFEM and GRASP data are straightforwardly determined with the procedure of section II B. With the parameters $\beta_0 = 10^{-2}$ and $\gamma = 1.4$, all the HELFEM and GRASP data are fit by a common set of 26 and 25 parameters, respectively, where the fit for each element typically uses only a fraction of the total set of parameters. The maximum fitting errors are $\tau = 1.68 \times 10^{-3}$ for Dy and $\tau = 1.22 \times 10^{-4}$ for Og for the HELFEM and GRASP fits, respectively.

Increasing the spacing to $\gamma = 1.8$, the HELFEM and GRASP data are fit by a common set of 17 and 13 parameters, respectively, each fit again using a subset of the common parameters. The maximum fitting errors are $\tau = 5.68 \times 10^{-3}$ for Lr and $\tau = 4.27 \times 10^{-3}$ for No for the HELFEM and GRASP potentials, respectively. The fitted potentials are available as part of the supplementary material, in both DIRAC and GAUSSIAN'94 basis set format.

| Potential | Mean error (E_h) |
|---------------------------------|----------------------|
| LDA@HF (ii), quadrature | 5.679 |
| GRASP, quadrature | 9.785 |
| optimized HF fit ^{a,b} | 11.531 |
| LDA@HF (ii), large fit | 11.743 |
| LDA@HF (ii), small fit | 11.836 |
| optimized LDA fit ^a | 12.244 |
| GRASP, large fit | 15.879 |
| GRASP, small fit | 16.699 |

TABLE III. Mean errors in the SAP guess energy for the transition metal complex database of ref. 44 at BP86/def2-QZVP level of theory. ^aFits from ref. 9. ^bThe HF potential was capped to charge neutrality.

V. MOLECULAR APPLICATIONS

A. Non-relativistic calculations

The accuracy of the fits can be compared to the quadrature results of section IV B; mean errors for error-function potentials as well as the GRASP quadrature guess are shown in table III. (The fitted guess, equation (3), was implemented in ERKALE for this comparison.) The SAP guess by quadrature is by far the most accurate; however, as the potential was chosen in section IV B to minimize the error for these calculations, this finding may be somewhat biased. The second-most accurate guess is afforded by the tabulated potential from GRASP, suggesting that the use of tabulated, fully numerical potentials as in ref. 1 is beneficial for accuracy: the integral on the Becke grid is essentially exact, which is why DFT calculations are tractable in the first place.

In contrast, the use of a Gaussian fit—whether it is explicitly optimized for molecules or not—poses limits on the accuracy of the guess. Interestingly, the errors for the present fits compare favorably with those for the optimized fits of ref. 9: the accuracy of the present unoptimized fits is close to that of the hand-optimized potentials of ref. 9. It is also interesting to note that the mean errors for all of the Gaussian-fit potentials (in the range of 11 to 16 kcal/mol) are close to those of the other choices for the fully numerical potential in the quadrature study in table II (10 to 16 kcal/mol).

The database is challenging for all the examined guesses, as errors of tens of E_h are observed for several molecules for every guess. The $\text{Sc}(\text{acac})_3$, $\text{Cu}(\text{acac})_2$, $\text{Ni}(\text{acac})_2$ complexes (acac = acetylacetonato) typically belong to the top four worst performers for all potentials.

B. Relativistic calculations

The fits of the GRASP potential derived in this work differ from the unpublished fits of DIRAC16 which were similarly based on LDA@HF, but also included a correla-

TABLE IV. Converged Dirac–Coulomb–Hartree–Fock energy E^{final} , and error in the large and small fit SAP guess energy $\Delta E^{\text{SAP}} = E^{\text{SAP}} - E^{\text{final}}$ for K_2 , CsCl , and UF_6 .

| Molecule | $E^{\text{final}} (E_h)$ | $\Delta E^{\text{SAP}}_{\text{large}} (E_h)$ | $\Delta E^{\text{SAP}}_{\text{small}} (E_h)$ |
|---------------|--------------------------|----------------------------------------------|----------------------------------------------|
| K_2 | −1203.033795 | 0.075046 | 0.070591 |
| CsCl | −8248.076864 | 0.145937 | 0.189300 |
| UF_6 | −28656.637434 | 0.438916 | 0.593749 |

tion contribution in the potential from the Vosko–Wilk–Nusair functional.⁴⁹ Moreover, an accurate, but computationally unoptimized fit to 30 functions with $\beta_0 = 10^{-2}$ and $\gamma = \sqrt{2}$ was used in DIRAC16. The fits of the present work are both more economical in terms of number of functions, as well as more accurate due to the exact adherence to the sum rule of equation (10) and the use of the complementary error function basis with analytical overlap. Although the present fits are smaller and do not include a correlation potential, the number of iterations needed to converge Hartree–Fock calculations remains similar, illustrating again the minor importance of the correlation functional for the starting potential as well as the small effect on self-consistent field convergence arising from minor changes to the atomic potential.

As an example, we show three illustrative cases for the performance of the SAP starting potentials. The K_2 dimer with an internuclear separation of 4.0 Å probes the long-range part of the potential, CsCl with a bond distance of⁵⁰ 2.906 Å represents a prototypical ionic bond, and the octahedral UF_6 molecule with an U–F distance of⁵¹ 1.996 Å tends to converge onto a higher-lying SCF solution with other starting procedures. The all-electron Dirac–Coulomb–Hartree–Fock calculations used the triple zeta basis sets developed by Dyall,^{52–54} with the default approximation of neglecting the (SS|SS) small-component Coulomb integrals.⁵⁵ All calculations with the SAP guess converge smoothly within 13 (K_2 and CsCl) or 18 (UF_6) iterations. As a further measure for the goodness of the guess, in table IV we compare the converged Dirac–Coulomb–Hartree–Fock energy to that of the first iteration, which is based on the orbitals that result from the diagonalization of the summed atomic potentials. The relatively small energy differences demonstrate the adequacy of even the small fit in the core and valence regions of the heavy atoms.

VI. SUMMARY AND DISCUSSION

The superposition of atomic potentials (SAP) guess¹ builds guess orbitals for electronic structure calculations from a simple sum of atomic effective potentials. We have compared atomic effective potentials from density functional and optimized effective potential calculations, and found their differences to be relatively small if the con-

figuration is fixed. Our results suggest that atomic local density exchange potentials should offer a good starting point for electronic structure calculations. We have also compared the local density exchange potentials arising from different choices for the atomic configuration, and found also these differences to be small. Due to this, it is our belief that any reasonable choice for the reference atomic configuration should yield suitable starting guesses; minimal-energy Hartree–Fock configurations were used in the present work.

We have pointed out that the SAP guess can be easily implemented in Gaussian-basis quantum chemistry programs by fitting the fully numerical, complete-basis-set-limit radial effective potentials in terms of error functions. We have described a robust method for forming such fits, and reported two sets of fits at two levels of accuracy available in the supplementary material, consisting of a common set of 17 and 26 s -type primitives, respectively, which are suitable for inclusion in electronic structure programs. Fits were formed both at the non-relativistic and fully relativistic levels of theory to suit the needs of all applications. As the fits consist of just one highly contracted s function, the computation of the resulting matrix elements as three-center two-electron integrals is extremely rapid even in large orbital basis sets.

The most commonly used initial guess nowadays is the superposition of atomic densities (SAD),^{56,57} in which a molecular calculation is initialized by a block-diagonal density matrix arising from a set of atomic calculations. The SAP guess is more aesthetically pleasing than SAD: SAP yields guess orbitals straight away, whereas SAD requires a full Fock matrix build from the non-idempotent guess density matrix, which can then be diagonalized to yield orbitals. In SAP, in contrast, the guess orbitals are obtained by diagonalizing the approximate one-electron Hamiltonian, in which the molecular potential is estimated directly as a superposition of pretabulated atomic potentials. The matrix elements necessary for SAP can be easily implemented by quadrature as in ref. 1; alternatively, as discussed in the present work, error-function fits to the atomic potentials allow reformulating the guess in terms of two-electron integrals in Gaussian-basis programs.

Despite their significant formal difference, the SAD and SAP approaches are quite similar at the complete basis set limit. In either case, the Coulomb part of the potential will be the same, as it is linear in the density: the Coulomb potential arising from the sum of spherically symmetric atomic densities is the same as the sum of spherically symmetric atomic Coulomb potentials. However, the situation is trickier for the exchange. Although the exact exchange operator is linear in the density matrix, the corresponding local scalar potential may behave discontinuously in the number of electrons.⁵⁸ Because of this, the approaches can be better contrasted within a density functional approximation: SAD yields a local ex-

change potential

$$V_x^{\text{SAD}}(\mathbf{r}) \propto - \left[\sum_A n_A(\mathbf{r}) \right]^{1/3} \quad (17)$$

whereas SAP yields

$$V_x^{\text{SAP}}(\mathbf{r}) \propto - \sum_A [n_A(\mathbf{r})]^{1/3}. \quad (18)$$

This appears to suggest that SAP is more attractive than SAD in molecules, meaning that SAD and SAP can always be expected to reproduce different results—even at the complete basis set limit. (Note that since generalized gradient approximation (GGA) and meta-GGA functionals build on top of the local exchange functional, a similar argument should also hold for them.) Although in many cases both SAD and SAP will lead to rapid convergence to the same ground-state in a self-consistent field calculation, systems with challenging electronic structures may exhibit several physical solutions of different symmetry or charge localization. Access to different types of guesses is extremely helpful in cases where a single guess does not perform adequately. Although several programs offer simple choices to SAD, such as the core Hamiltonian a.k.a. one-electron guess, these choices may be of extremely poor accuracy for large systems in contrast to SAD and SAP that both account for screening effects in heavy atoms.¹ The present fitted atomic potentials facilitate the inclusion of the SAP guess in commonly-used Gaussian-basis quantum chemistry programs, thereby introducing a new class of accurate initial guesses that may aid studies on challenging systems.

SUPPLEMENTARY MATERIAL

See supplementary material for the small ($\gamma = 1.8$) and large ($\gamma = 1.4$) fits to the HELFEM and GRASP potentials, in both DIRAC and GAUSSIAN’94 format.

ACKNOWLEDGMENTS

This work has been supported by the Academy of Finland (Suomen Akatemia) through project number 311149. Computational resources provided by CSC – It Center for Science Ltd (Espoo, Finland) and the Finnish Grid and Cloud Infrastructure (persistent identifier urn:nbn:fi:research-infras-2016072533) are gratefully acknowledged.

¹S. Lehtola, “Assessment of Initial Guesses for Self-Consistent Field Calculations. Superposition of Atomic Potentials: Simple yet Efficient,” *J. Chem. Theory Comput.* **15**, 1593–1604 (2019), arXiv:1810.11659.

²A. E. S. Green, D. L. Sellin, and A. S. Zachor, “Analytic Independent-Particle Model for Atoms,” *Phys. Rev.* **184**, 1–9 (1969).

- ³J. E. Whalen and A. E. S. Green, “Analytic Independent Particle Model for Molecules,” *Am. J. Phys.* **40**, 1484–1489 (1972).
- ⁴F. Nazari and J. L. Whitten, “Prediction of many-electron wavefunctions using atomic potentials,” *J. Chem. Phys.* **146**, 194109 (2017).
- ⁵J. L. Whitten, “Prediction of many-electron wavefunctions using atomic potentials: Refinements and extensions to transition metals and large systems,” *J. Chem. Phys.* **150**, 034107 (2019), arXiv:1812.11820.
- ⁶J. L. Whitten, “Prediction of many-electron wavefunctions using atomic potentials: extended basis sets and molecular dissociation,” *Phys. Chem. Chem. Phys.* **21**, 21541–21548 (2019).
- ⁷S. Lehtola, “A review on non-relativistic, fully numerical electronic structure calculations on atoms and diatomic molecules,” *Int. J. Quantum Chem.* **119**, e25968 (2019), arXiv:1902.01431.
- ⁸S. Lehtola, “Fully numerical calculations on atoms with fractional occupations and range-separated exchange functionals,” *Phys. Rev. A* **101**, 012516 (2020), arXiv:1908.02528.
- ⁹D. N. Laikov and K. R. Briling, “Atomic effective potentials for starting molecular electronic structure calculations,” *Theor. Chem. Acc.* **139**, 17 (2020), arXiv:1902.03212.
- ¹⁰S. Lehtola, “Superposition of Atomic Potentials: a simple yet efficient orbital guess for self-consistent field calculations,” *arXiv Prepr.* 1810.11659v1 (2018), arXiv:1810.11659.
- ¹¹O. Vahtras, J. Almlöf, and M. W. Feyereisen, “Integral approximations for LCAO-SCF calculations,” *Chem. Phys. Lett.* **213**, 514–518 (1993).
- ¹²L. Visscher and K. G. Dyall, “Dirac-Fock atomic electronic structure calculations using different nuclear charge distributions,” *At. Data Nucl. Data Tables* **67**, 207–224 (1997).
- ¹³D. Andrae, “Finite nuclear charge density distributions in electronic structure calculations for atoms and molecules,” *Phys. Rep.* **336**, 413–525 (2000).
- ¹⁴P. Hohenberg and W. Kohn, “Inhomogeneous Electron Gas,” *Phys. Rev.* **136**, B864–B871 (1964).
- ¹⁵W. Kohn and L. J. Sham, “Self-Consistent Equations Including Exchange and Correlation Effects,” *Phys. Rev.* **140**, A1133–A1138 (1965).
- ¹⁶A. D. Becke, “A multicenter numerical integration scheme for polyatomic molecules,” *J. Chem. Phys.* **88**, 2547–2553 (1988).
- ¹⁷S. Lehtola, “ERKALE – HF/DFT from Hel,” (2018).
- ¹⁸J. Lehtola, M. Hakala, A. Sakko, and K. Hämäläinen, “ERKALE – A flexible program package for X-ray properties of atoms and molecules,” *J. Comput. Chem.* **33**, 1572–1585 (2012).
- ¹⁹R. M. Parrish, L. A. Burns, D. G. A. Smith, A. C. Simmonett, A. E. DePrince, E. G. Hohenstein, U. Bozkaya, A. Y. Sokolov, R. Di Remigio, R. M. Richard, J. F. Gonthier, A. M. James, H. R. McAlexander, A. Kumar, M. Saitow, X. Wang, B. P. Pritchard, P. Verma, H. F. Schaefer, K. Patkowski, R. A. King, E. F. Valeev, F. A. Evangelista, J. M. Turney, T. D. Crawford, and C. D. Sherrill, “Psi4 1.1: An Open-Source Electronic Structure Program Emphasizing Automation, Advanced Libraries, and Interoperability,” *J. Chem. Theory Comput.* **13**, 3185–3197 (2017).
- ²⁰S. Lehtola, “HelFEM – Finite element methods for electronic structure calculations on small systems,” (2018).
- ²¹S. Lehtola, “Fully numerical Hartree-Fock and density functional calculations. I. Atoms,” *Int. J. Quantum Chem.* **119**, e25945 (2019), arXiv:1810.11651.
- ²²S. Lehtola, “Fully numerical Hartree-Fock and density functional calculations. II. Diatomic molecules,” *Int. J. Quantum Chem.* **119**, e25944 (2019), arXiv:1810.11653.
- ²³E. van Lenthe, E. J. Baerends, and J. G. Snijders, “Relativistic regular two-component Hamiltonians,” *J. Chem. Phys.* **99**, 4597 (1993).
- ²⁴“ADF 2019.3, SCM, Theoretical Chemistry, Vrije Universiteit, Amsterdam, The Netherlands,” (2019).
- ²⁵S. F. Boys, “Electronic Wave Functions. I. A General Method of Calculation for the Stationary States of Any Molecular System,” *Proc. R. Soc. A Math. Phys. Eng. Sci.* **200**, 542–554 (1950).

- ²⁶L. E. McMurchie and E. R. Davidson, “One- and two-electron integrals over cartesian Gaussian functions,” *J. Comput. Phys.* **26**, 218–231 (1978).
- ²⁷S. Obara and A. Saika, “Efficient recursive computation of molecular integrals over Cartesian Gaussian functions,” *J. Chem. Phys.* **84**, 3963 (1986).
- ²⁸R. Ahlrichs, “Efficient evaluation of three-center two-electron integrals over Gaussian functions,” *Phys. Chem. Chem. Phys.* **6**, 5119 (2004).
- ²⁹P.-O. Löwdin, “Quantum theory of cohesive properties of solids,” *Adv. Phys.* **5**, 1–171 (1956).
- ³⁰S. Lehtola, F. Blockhuys, and C. V. Van Alsenoy, “An Overview of Self-Consistent Field Calculations Within Finite Basis Sets,” *Molecules* **25**, 1218 (2020), arXiv:1912.12029.
- ³¹D. F. Feller and K. Ruedenberg, “Systematic approach to extended even-tempered orbital bases for atomic and molecular calculations,” *Theor. Chim. Acta* **52**, 231–251 (1979).
- ³²S. Lehtola, “Polarized universal hydrogenic Gaussian basis sets from one-electron ions,” (2020), arXiv:2001.04224.
- ³³O. Fossgaard and T. Saue, “LDA potential implementation in GRASP, unpublished,” (2002).
- ³⁴K. G. Dyall, I. P. Grant, C. T. Johnson, F. A. Parpia, and E. P. Plummer, “GRASP: A general-purpose relativistic atomic structure program,” *Comput. Phys. Commun.* **55**, 425–456 (1989).
- ³⁵E. Engel and S. H. Vosko, “Accurate optimized-potential-model solutions for spherical spin-polarized atoms: Evidence for limitations of the exchange-only local spin-density and generalized-gradient approximations,” *Phys. Rev. A* **47**, 2800–2811 (1993).
- ³⁶J. B. Krieger, Y. Li, and G. J. Iafrate, “Exact relations in the optimized effective potential method employing an arbitrary $E_{xc}[\psi_{i\sigma}]$,” *Phys. Lett. A* **148**, 470–474 (1990).
- ³⁷F. Bloch, “Bemerkung zur Elektronentheorie des Ferromagnetismus und der elektrischen Leitfähigkeit,” *Zeitschrift für Phys.* **57**, 545–555 (1929).
- ³⁸P. A. M. Dirac, “Note on Exchange Phenomena in the Thomas Atom,” *Math. Proc. Cambridge Philos. Soc.* **26**, 376–385 (1930).
- ³⁹J. P. Perdew, K. Burke, and M. Ernzerhof, “Generalized Gradient Approximation Made Simple,” *Phys. Rev. Lett.* **77**, 3865–3868 (1996).
- ⁴⁰E. Engel and S. H. Vosko, “Exact exchange-only potentials and the virial relation as microscopic criteria for generalized gradient approximations,” *Phys. Rev. B* **47**, 13164–13174 (1993).
- ⁴¹M.-C. Kim, E. Sim, and K. Burke, “Ions in solution: Density corrected density functional theory (DC-DFT),” *J. Chem. Phys.* **140**, 18A528 (2014), arXiv:1403.1671.
- ⁴²S. Vuckovic, S. Song, J. Kozłowski, E. Sim, and K. Burke, “Density Functional Analysis: The Theory of Density-Corrected DFT,” *J. Chem. Theory Comput.* **15**, 6636–6646 (2019), arXiv:1908.05721.
- ⁴³J. P. Perdew, J. Sun, A. Ruzsinszky, P. D. Mezei, and G. I. Csonka, “Why Density Functionals Should Not Be Judged Primarily by Atomization Energies,” *Period. Polytech. Chem. Eng.* **60**, 2–7 (2016).
- ⁴⁴M. Bühl and H. Kabrede, “Geometries of Transition-Metal Complexes from Density-Functional Theory,” *J. Chem. Theory Comput.* **2**, 1282–1290 (2006).
- ⁴⁵A. D. Becke, “Density-functional exchange-energy approximation with correct asymptotic behavior,” *Phys. Rev. A* **38**, 3098–3100 (1988).
- ⁴⁶J. Perdew, “Density-functional approximation for the correlation energy of the inhomogeneous electron gas,” *Phys. Rev. B* **33**, 8822–8824 (1986).
- ⁴⁷F. Weigend, F. Furche, and R. Ahlrichs, “Gaussian basis sets of quadruple zeta valence quality for atoms H–Kr,” *J. Chem. Phys.* **119**, 12753 (2003).
- ⁴⁸F. Weigend, “Accurate Coulomb-fitting basis sets for H to Rn,” *Phys. Chem. Chem. Phys.* **8**, 1057–65 (2006).
- ⁴⁹S. H. Vosko, L. Wilk, and M. Nusair, “Accurate spin-dependent electron liquid correlation energies for local spin density calculations: a critical analysis,” *Can. J. Phys.* **58**, 1200–1211 (1980).
- ⁵⁰P. J. Linstrom and W. G. Mallard, “NIST Chemistry WebBook, NIST Standard Reference Database Number 69, National Institute of Standards and Technology, Gaithersburg MD, 20899,” (2020).
- ⁵¹M. Kimura, V. Schomaker, D. W. Smith, and B. Weinstock, “Electron-Diffraction Investigation of the Hexafluorides of Tungsten, Osmium, Iridium, Uranium, Neptunium, and Plutonium,” *J. Chem. Phys.* **48**, 4001–4012 (1968).
- ⁵²K. G. Dyall, “Relativistic double-zeta, triple-zeta, and quadruple-zeta basis sets for the actinides Ac–Lr,” *Theor. Chem. Acc.* **117**, 491–500 (2006).
- ⁵³K. G. Dyall, “Relativistic double-zeta, triple-zeta, and quadruple-zeta basis sets for the 4s, 5s, 6s, and 7s elements,” *J. Phys. Chem. A* **113**, 12638–44 (2009).
- ⁵⁴K. G. Dyall, “Relativistic double-zeta, triple-zeta, and quadruple-zeta basis sets for the light elements H–Ar,” *Theor. Chem. Acc.* **135**, 128 (2016).
- ⁵⁵L. Visscher, “Approximate molecular relativistic Dirac—Coulomb calculations using a simple Coulombic correction,” *Theor. Chim. Acta* **98**, 68–70 (1997).
- ⁵⁶J. Almlöf, K. Faegri, and K. Korsell, “Principles for a direct SCF approach to LCAO-MO ab-initio calculations,” *J. Comput. Chem.* **3**, 385–399 (1982).
- ⁵⁷J. H. Van Lenthe, R. Zwaans, H. J. J. Van Dam, and M. F. Guest, “Starting SCF calculations by superposition of atomic densities,” *J. Comput. Chem.* **27**, 926–32 (2006).
- ⁵⁸M. J. P. Hodgson, E. Kraisler, A. Schild, and E. K. U. Gross, “How Interatomic Steps in the Exact Kohn–Sham Potential Relate to Derivative Discontinuities of the Energy,” *J. Phys. Chem. Lett.* **8**, 5974–5980 (2017), arXiv:1706.00586.